Development of Biosensor Using liquid Crystal in Anodic Aluminum Oxide for the Detection of Pollutants and Pathogens

Danish Tahir	**Regn. No. NUST2013BSCME0499899213F**
Syed Irfan Raies	**Regn. No. NUST2013BSCME0566799213F**
Asim Iltaf	**Regn. No. NUST2013BSCME0668099213F**

This report is submitted as a FYP thesis in partial fulfillment of the requirement for the degree of

(BE in Materials Engineering)

Supervisor: Dr. Haris Masood Ansari

Department of Materials Engineering

School of Chemical and Materials Engineering

National University of Sciences and Technology

June, 2017

Certificate

This is to certify that work in this thesis has been carried out by **Mr. Danish Tahir, Mr. Syed Irfan Raies and Mr. Asim Iltaf** and completed under my supervision in corrosion laboratory, school of chemical and materials engineering, National University of Sciences and Technology, H-12, Islamabad, Pakistan.

Supervisor：Dr. Haris Ansari
Department of Materials Engineering
School of Chemical & Materials Engineering,
National University of Sciences and Technology, Islamabad

Co-supervisor：Dr. Zakir Hussain
Department of Materials Engineering
School of Chemical & Materials Engineering,
National University of Sciences and Technology, Islamabad

Submitted through:

HoD：
Department of Materials Engineering
School of Chemical & Materials Engineering,
National University of Sciences and Technology, Islamabad

Dean：
Department of Materials Engineering
School of Chemical & Materials Engineering,
National University of Sciences and Technology, Islamabad

Dedication

“We would like to dedicate our thesis to our families, friends and to our beloved teachers”

Acknowledgment

We would like to thank the teachers and mentor-teachers in our department who assisted us with this project whose willingness to give feedback made this research very enjoyable experience. We would also like to acknowledge and thank our school SCME for allowing us to conduct our research and providing any assistance which we requested.

We would slso like to thank our supervisor Dr. Haris Ansari and co-supervisor Dr. Zakir Husssain for their immense support and encouragement throughout this project. We also recognize the cooperation of SCME technical staff specially Mr. Shamshuddin.

Abstract

Anodized aluminum oxide (AAO) channels can replace expensive TEM gold grids as sensing chambers for liquid crystal based sensing applications. In this project aluminum foil will be used to fabricate AAO channels via anodization because of cost effectiveness and ease of fabrication. Stepwise anodization was performed by varying the voltage and temperature to achieve the desired pore diameter for incorporation of liquid crystal in these channels for bio-sensing applications. Close-packed Nano-pores were produced by varying different process parameters of anodization process i.e. time of anodization, type of electrolyte being used, temperature of electrolyte, purity of aluminum foil and voltage being used. The next part is to grow liquid crystal molecules in those Nano-pores and use them for bio-sensing applications.

Table of Contents

Acknowledgment i

Abstract ii

List of Figures vi

List of Tables viii

Abbreviations ix

Chapter-1: Introduction 1

1.1.Aluminum Anodization 1

1.2.Parameters Of Anodization Effects On Aluminum 2

1.3.Electrochemical Reactions 3

- 1.3.1. Electro-Etching 3
- 1.3.2. Electro-deposition 4
- 1.3.3. Anodization 5
- 1.3.4. Electro-polishing 5
- 1.3.5. Corrosion Protection 6

1.4.Liquid Crystals 6

- 1.4.1. Liquid Crystal Phases 6
  - 1.4.1.1. Metallotropic 6
  - 1.4.1.2. Thermotropic 7
    - I) Nematic Phase 7
    - II) Smectic Phase 7
    - III) Cholestric Phase 7
  - 1.4.1.3. Lyotropic 7
- 1.4.2. Liquid Crystals Alignment 7
  - 1.4.2.1. Homogenous Alignment 7
  - 1.4.2.2. Homeotropic Alignment 8

1.5.Liquid Crystals As Sensors 8

1.6.Whatman® Anodisc Inorganic Membranes 9

1.7.Problem Statement 9

Chapter-2: Literature Review 10

2.1.Two step Anodization 11
2.2.Pore formation process 12
  2.2.1. Oxide formation 13
  2.2.2. Initiation of pores 13
  2.2.3. Formation of pore 13
  2.2.4. Growth of pores 14
2.3.Processing parameters 14
  2.3.1. Pore size 14
  2.3.2. Inter-pore distance 15
  2.3.3. Thickness 16
2.4.Applications Overview 17
Chapter 3: Experimental Procedure 18
3.1.Electrochemical Anodization setup 18
  3.1.1. Power Supply 18
  3.1.2. Digital Multi-meter 18
  3.1.3. Computer Interface 19
  3.1.4. Magnetic Stirrer 20
  3.1.5. Recirculating Chiller 20
  3.1.6. Anode 21
  3.1.7. Cathode 21
  3.1.8. Electrolyte 21
    3.1.8.1 0.3 M oxalic acid: 21
    3.1.8.2 5 vol. percent phosphoric acid: 21
3.2.Experiment Steps 22
  3.2.1 Sample Preparation 22
    3.2.1.1 Annealing 22
    3.2.1.2. Electro-polishing 22
    3.2.1.3. First Anodization 22
    3.2.1.4. Pore Widening 22
    3.2.1.5. 2nd Anodization 22
3.3.Experimental Scheme 22

3.4.Anodization Bath 23
Chapter 4: Results and Discussions 24
4.1.SEM images and current profiles 24
  4.1.1. Surface analysis of AAO obtained at 60V 24
  4.1.2. Surface analysis of AAO anodized at 50V 26
  4.1.3. Sample analysis of AAO at 70V 28
  4.1.4. Surface analysis of AAO obtained at 25V 31
  4.1.5. Surface Analysis of AAO obtained at 40V 32
  4.1.6. Surface Analysis of AAO obtained at 40V 34
4.2.Future perspective 35
5.Conclusions 36
6.References 37

List of Figures

Figure 1.1 (a) Schematic of AAO structure developed by electrochemical anodization of Aluminum (b) Self-ordering voltage and inter-pore distance of AAO produced within these electrolytes i.e. sulfuric, oxalic and phosphoric. (c) (Top) shows the SEM cross-sectional view of the anodic aluminum oxide membrane formed by MA (0.3 M H2C2O4, 1 LC, and 40 V) and (bottom) by HA (at 140 V) for 2 hours (insets: Shows SEM top view of pore structure)…………………………………………………………………………………...1

Figure 1.2 Schematic shows the AAO structure and the main applications of nanostructured material…………………………………………………………………………………….2

Figure 1.3 Relationship between the voltage and the resulting cell diameter, pore diameter…………………………………………………………………………………...3

Figure 1.4 Schematic of Electro-etching Process……………………………………….....4

Figure 1.5 Schematic of Electro-deposition……………………………………………....4

Figure 1.6 Schematic of Anodization Process…………………………………………......5

Figure 1.7 Schematic of Electro-etching Process…………………………………………6

Figure 1.8 Schematic of the LC-based sensor (a) sensing mechanism of the LCs reorientation associated with the reaction of dodecyl -d-glucopyranoside by cellulase at the aqueous/LC interface: perpendicular (b) planar (c) states. The corresponding images combined to the orientation of LCs: black (d) bright (e) appearances………………………………………8

Figure 1.9 Principal of LC-based sensor (a) 5CB partially aligned in gold grids, also showing light transmission; (b) optical image of partially aligned 5CB observed under optical microscope; (c) 5CB fully aligned in gold grids, also showing light blocking; (d) Optical image of fully aligned 5CB observed under optical microscope…………………………………………..9

Figure 2.1 SEM images of AAO immersed in 5 wt% H3PO4 for 35 min at 40oC. (a) Top view. (b) Bottom view…………………………………………………………………………...10

Figure 2.2 Schematic representations showing the fabrication of porous alumina by two step anodization. (A) Formation of porous alumina after first anodization; (B) this part shows the removal of porous alumina formed in first anodization; (C) Formation of perfect and ordered pores by using second anodization process; (D) Free-standing porous anodic alumina; (E) Structure obtained after electrical detachment of porous anodic alumina……………………………………………………………………………….....11

Figure 2.3 Schematic representation showing the kinetics of anodization process………....12

Figure 2.4 Schematic showing the stages of pore formation…………………………..........13

Figure 2.5 Initial pore formation……………………………………………………………14

Figure 2.6 Variation of membrane thickness with respect to time……………………..........17

Figure 3.1 Power Supply…………………………………………………………….........18

Figure 3.2 Uni-Trend T-60 Ampere Digital Multi-meter…………………………….............19

Figure 3.3 Computer Interface Screen…………………………………………………........20

Figure 3.4 Digital hotplate MSH20D wise magnetic stirrer……………………………........20

Figure 3.5 Haake F3 Recirculating Chiller…………………………………………………..21

Figure 3.6 Experimental Setup…………………………………………………………........24

Figure 4.1 SEM image of anodized aluminum foil, anodized at 60V and in 5 Vol% phosphoric acid and image is taken at a magnification of 5000X……………………………………..26

Figure 4.2 SEM image at magnification of 40000X……………………………………........27

Figure 4.3 SEM micrograph of AAO at a magnification of 30000X………………….........28

Figure 4.4 SEM micrograph at a magnification of 40000X…………………………….....29

Figure 4.5 SEM image of burnt sample at a magnification of 5000X……………………....30

Figure 4.6 SEM image of sample at magnification of 30000X……………………….........31

Figure 4.7 SEM micrographs for anodization of aluminum foil performed at 25V in 0.3M oxalic acid at magnification of 50000X…………………………………………………….......32

Figure 4.8 Current profile…………………………………………………………………..33

Figure 4.9 SEM micrograph of anodization of Aluminum foil at 40V in 0.3 M oxalic acid ……………………………………………………………………………………………...34

Figure 4.10 Burnt sample profile after first anodization…………………………………...34

Figure 4.11 SEM micrograph for anodization of Aluminum foil at 40V, in 0.3 M oxalic acid and at the magnification of 50000X…………………………………………………………35

Figure 4.12 Burnt sample profile after 2nd anodization…………………………………....36

List of Tables

Table 2.1……………………………………………………………………………14

Table 2.2……………………………………………………………………………15

Table 2.3……………………………………………………………………………15

Table 2.4……………………………………………………………………………16

Table 3.1……………………………………………………………………………23

Table 4.1……………………………………………………………………………25

Table 4.2……………………………………………………………………………27

Table 4.3……………………………………………………………………………29

Table 4.4……………………………………………………………………………32

Table 4.5……………………………………………………………………………33

Table 4.6……………………………………………………………………………35

Abbreviations

AAO	Anodic Aluminum Oxide
SEM	Scanning Electron Microscope
DC	Direct Current
DMM	Digital Multi-meter
AO	Anodization in Oxalic Acid
AP	Anodization in Phosphoric Acid
LC	Liquid Crystals

Chapter-1

Introduction

1.1. Aluminum Anodization

Aluminum anodization is a two-step electrochemical process in which an aluminum oxide layer is formed on the aluminum which was originally used [1, 2]. The aluminum oxide contains hexagonal ordered pores as a result of anodization process. Voltage is applied to aluminum foil or sheet in acidic electrolyte which leads to formation of aluminum oxide layer. The hexagonal pores structure which is also called anodized aluminum oxide (AAO). The structure of AAO is a close-packed hexagonal shape array of Nano-pores which are parallel to each other and perpendicular to the surface of the underlying Aluminum substrates [3, 4].

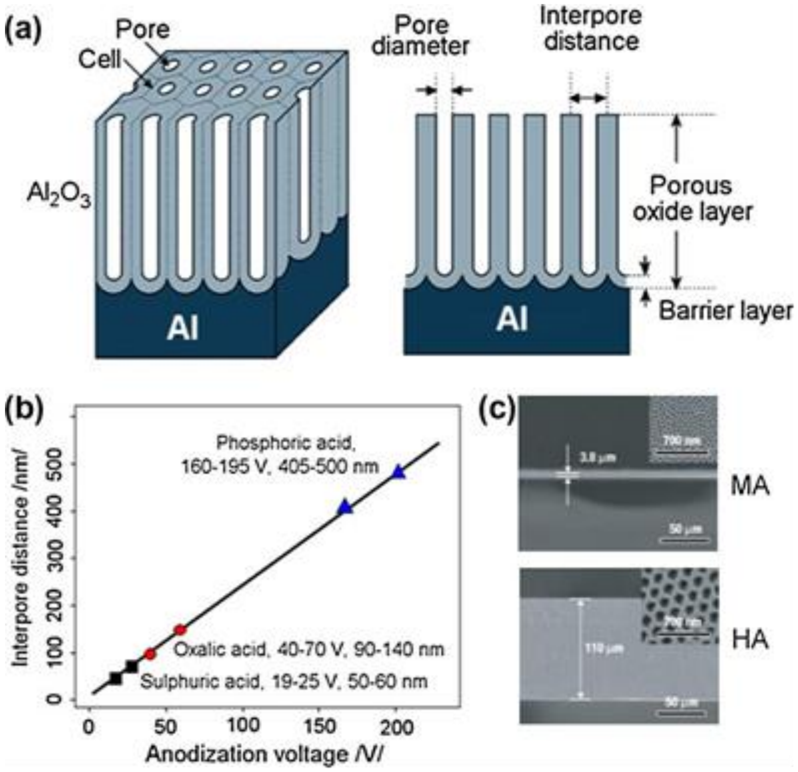

Figure 1.1 (a) Schematic of AAO structure developed by electrochemical anodization of Aluminum (b) Self-ordering voltage and inter-pore distance of AAO produced within these electrolytes i.e. sulfuric, oxalic and phosphoric. (c) (Top) shows the SEM cross-sectional view of the anodic aluminum oxide membrane formed by MA (0.3 M $H_2C_2O_4$, 1 LC, and 40 V) and (bottom) by HA (at 140 V) for 2 hours (insets: Shows SEM top view of pore structure) [3].

The pore formation of AAO film was affected by several parameters, such as the anodization voltage, concentration and nature of acid solutions, temperature of electrolyte and the first anodization time [5]. Nano-porous anodic aluminum oxide (AAO) gained exposure recently for use as a membrane in applications such as gas separation, drug delivery, and bone fixation [6].

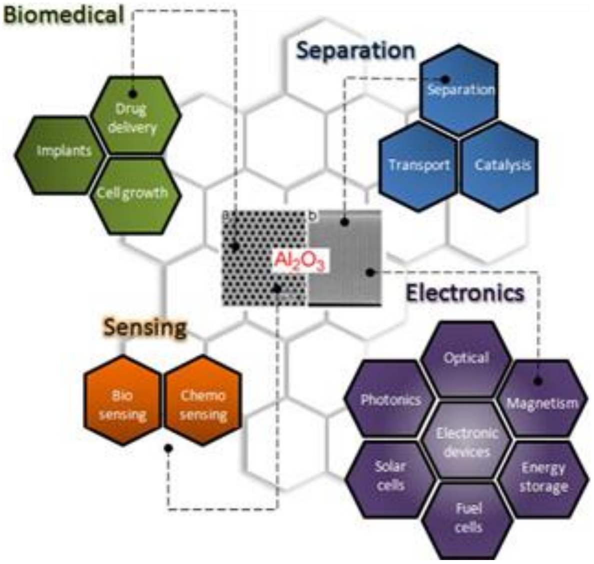

Figure 1.2 Schematic shows the AAO structure and the main applications of nanostructured material [3].

1.2. Parameters Of Anodization Effects On Aluminum

Aluminum can be anodized in various types of acid solutions i.e. oxalic acid, phosphoric acid, and sulfuric acid [6, 7]. The required pore size and the final application in which AAO has to be used decide the type of acid solution [5]. Concentrated acid solutions gives bigger size pores while small pores of AAO can be obtained using sulfuric acid. Anodization done at constant voltage with dilute acidic electrolyte is known as potentiostatic anodization while the anodization which is performed at constant current is known as galvanostatic anodization. The working voltage for oxalic acid is generally in the range of 20-40V and for phosphoric acid it is 60-195V. Working at high voltage may result in local heat generation at aluminum surface which can be avoided by using low temperature, but working at low temperature result in compact, thick and hard AAO layer. Anodic aluminum oxide pore size and channels depth are greatly affected by all the parameter and the final morphology of channels depends upon varying these parameters i.e. temperature, voltage, anodization time and electrolyte type [5, 8]. Pretreatments of sample also play a significant role in anodization as improper pretreatments and handling of aluminum sample leads to generation of local heat on sample surface which initiates the burning of sample [9]. Besides all the parameters which affect AAO Pore size, voltage has linear relationship with aluminum oxide pore size. The effect of changing the voltage on pore diameter is evident in below figure.

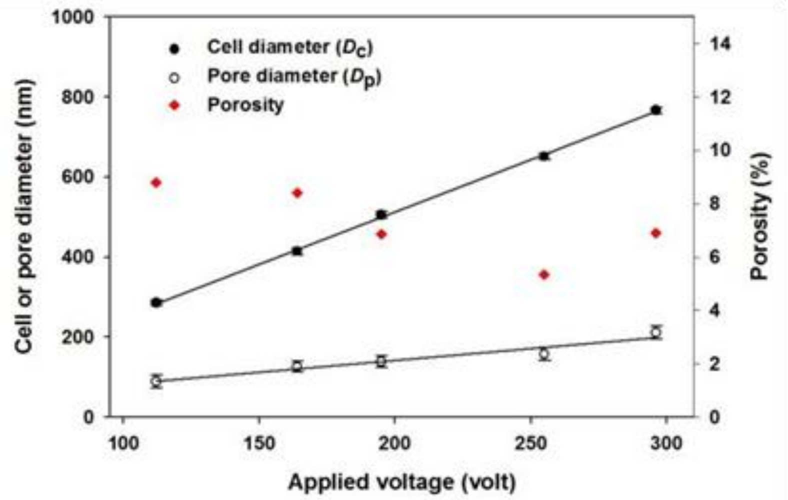

Figure 1.3 Relationship between the voltage and the resulting cell diameter, pore diameter [10].

1.3. Electrochemical Reactions

There are various electrochemical techniques which are currently being employed i.e. Electro-etching, Electro-polishing, Anodization, Corrosion protection setups and Electro-deposition. Electrochemical reaction occurs only in the presence of following four critical components which are responsible for the initiation and continuation of reaction [11]. These critical components are described below in detail.

- Electrolyte
- Cathode
- Anode
- A connection between cathode and anode for the flow of electrons.

1.3.1. Electro-Etching

Electro-etching is an electrochemical reaction in which the positive terminal of the power supply is connected with sample. An electrical connection is made between cathode and anode through which the electrons flow. The sample discharges positive ions towards electrolyte and the electrons moves through the electrical connection towards cathode. Electro-etching process is depicted clearly in below figure.

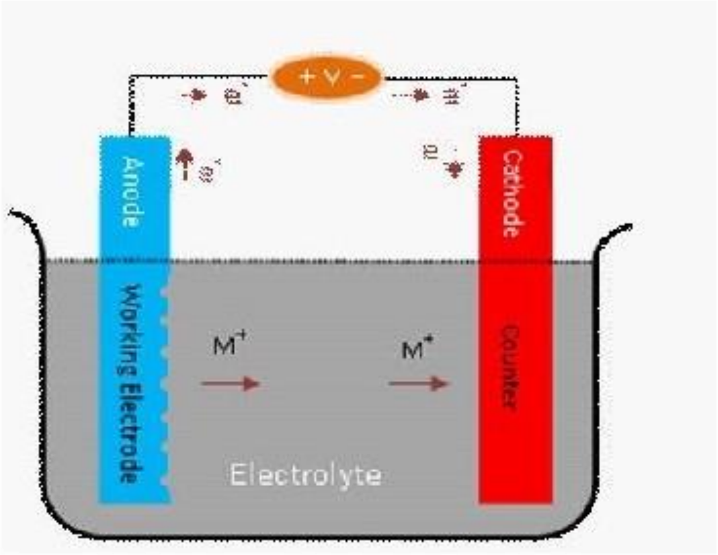

Figure 1.4 Schematic of Electro-etching Process [12].

1.3.2. Electro-deposition

In this type of electrochemical process, graphite or lead which is inert electrode are used as anode and the sample on which deposition has to be done act as cathode. The positive ions in the electrolyte are attracted towards cathode and get deposited on the sample surface. The anode doesn't participate in the reaction itself. Schematically electro-deposition is shown in below figure.

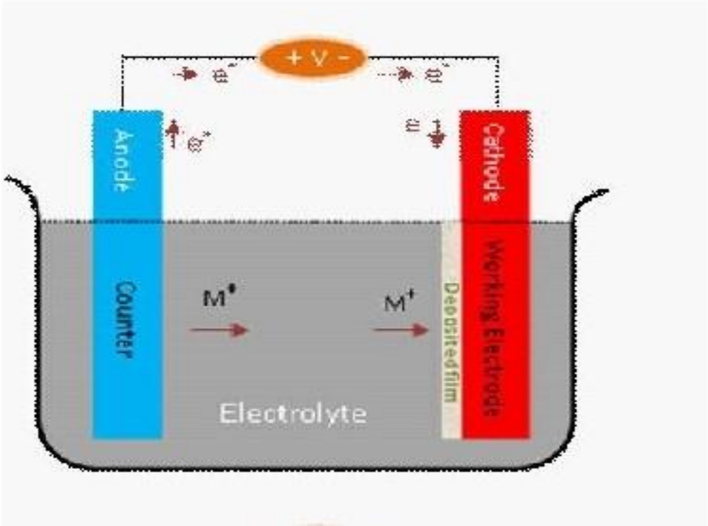

Figure 1.5 Schematic of Electro-deposition [12].

1.3.3. Anodization

This electrochemical process is used for forming oxide layer on sample such as aluminum oxide in case of aluminum. In this case working electrode is anode while the counter electrode is cathode. Electrons moves from anode to cathode through the electrical connection. The negative ions in the electrolyte are attracted towards anode on which oxide layer is formed. The schematic representation of anodization process is shown below.

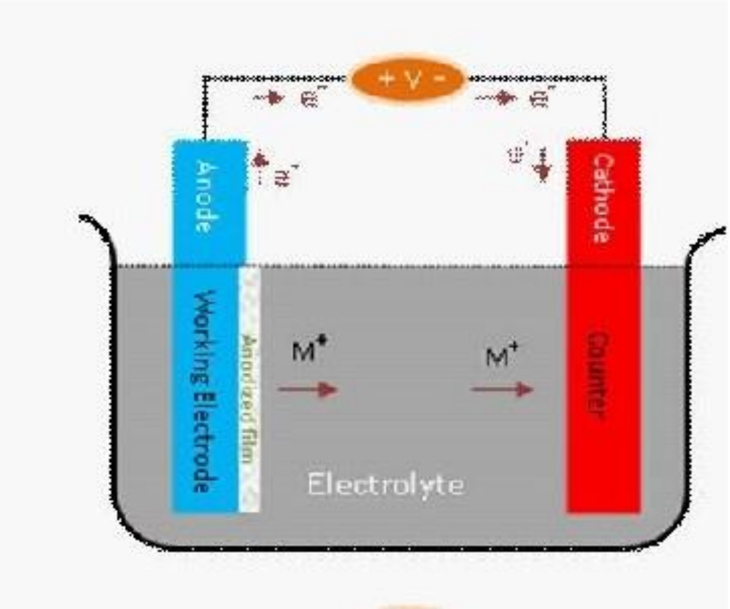

Figure 1.6 Schematic of Anodization Process [12].

1.3.4. Electro-polishing

Electro-polishing is an electrochemical process in which the working electrode is anode and counter electrode is cathode. In electro-polishing process the electrolyte used is concentrated acid in which the metallic surface of sample oxidizes and sample dissolves in the electrolyte. So in this way electro-polishing is achieved. The schematic below shows the mechanism of this process.

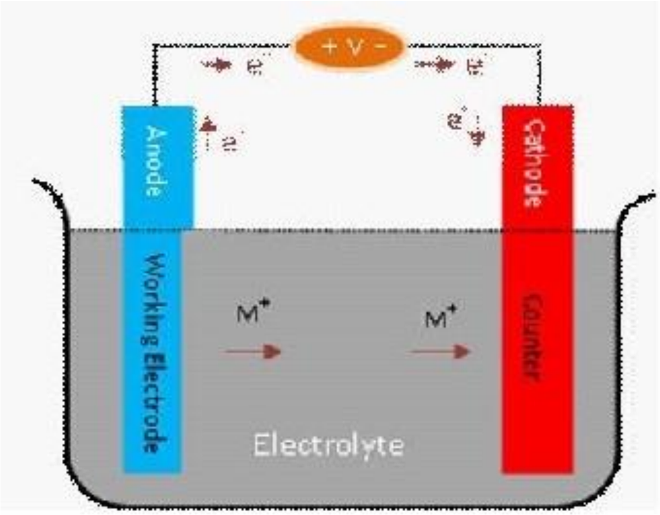

Figure 1.7 Schematic of Electro-etching Process [12].

1.3.5. Corrosion Protection

In this process the surface of metals is protected from degradation due to corrosion by making the surface of metals cathode of an electrochemical cell. The main types of corrosion protection are as follows:

- Impressed current cathodic protection
- Cathodic protection

1.4. Liquid Crystals

Liquid crystal is a unique material which flows like liquid but has some order of crystallinity or order in the arrangement of its atoms. This substance behaves like liquid as well as solid. It represents a kind of intermediate phase between solid and liquid as it has got the flow property of liquid and at the same time act like solid material. Liquid crystals have properties of liquid as well as solid such as anisotropy, magnetic properties, fluidity and optical properties. It is a state of matter which has some properties of liquid but behaves as solid as well.

1.4.1. Liquid Crystal Phases

Liquid crystals have different phases which are differentiated on various properties such as temperature, organic molecules, inorganic molecules and ordering. The main phases of liquid crystals are described below.

1.4.1.1. Metallotropic

Those liquid crystals which have organic-inorganic ratio of molecules at very low temperature are known as metallotropic liquid crystals [13].

1.4.1.2. Thermotropic

Different ranges of temperature define different types of liquid crystals as thermotropic is a kind of phase which depends heavily on temperature. By changing temperature, different phases of liquid crystals form. Thermotropic is further subdivided into other phases which are described below briefly [13].

I) Nematic Phase

It is a Greek word which means “Thread” because the liquid molecules in this phase align themselves into thread like orientation. Nematic is a transparent and translucent phase due to which polarization of liquid crystal occur [14].

II) Smectic Phase

Smectic is a Latin word which means “of soapy nature or to clean”. When this phase is observed at temperature lower than nematic phases, the layers are clearly well defined.

III) Cholestric Phase

The chiral molecules in liquid crystals makes make twist in the nematic phase which results into a twisted helical shape phase classified as cholesteric liquid crystal phase. There are certain layers which are quasi-nematic but they are at definite angles.

1.4.1.3. Lyotropic

In these types of liquid crystals the phase changes as a response of varying the temperature and concentration [13].

1.4.2. Liquid Crystals Alignment

Generally liquid Crystals have two types of alignment which are found in liquid crystal molecules [15]. These two types are described below briefly.

- Homogenous Alignment
- Homeotropic Alignment

1.4.2.1. Homogenous Alignment

When liquid crystal molecules align themselves in such a way that they become parallel with substrate molecules then this alignment is known as homogenous alignment [13].

1.4.2.2. Homeotropic Alignment

In this alignment the liquid crystal molecules align themselves perpendicular to the substrate [13].

1.5. Liquid Crystals As Sensors

Liquid crystals have responsive nature towards external light, voltage and other foreign molecules [7, 13]. This responsive nature of liquid crystal is used for different sensing applications. 5CB which is 4cyano-4pentyl-biphenyl ($C_{18}H_{18}N$) shows nematic mesophase, they are used in various applications such as in sensing and electro-optic display applications. N-dimethyl-N-octyl-N-3trimethoxy silyl propyl ammonium chloride (DMOAP) is usually used as surfactant to get homeotropic alignment [16]. Actually surfactant gives a layer of required alignment on glass substrate [13, 17]. The gold grid function is to provide chambers for liquid crystals. Liquid crystals films are not attached and they are independent in each grid.

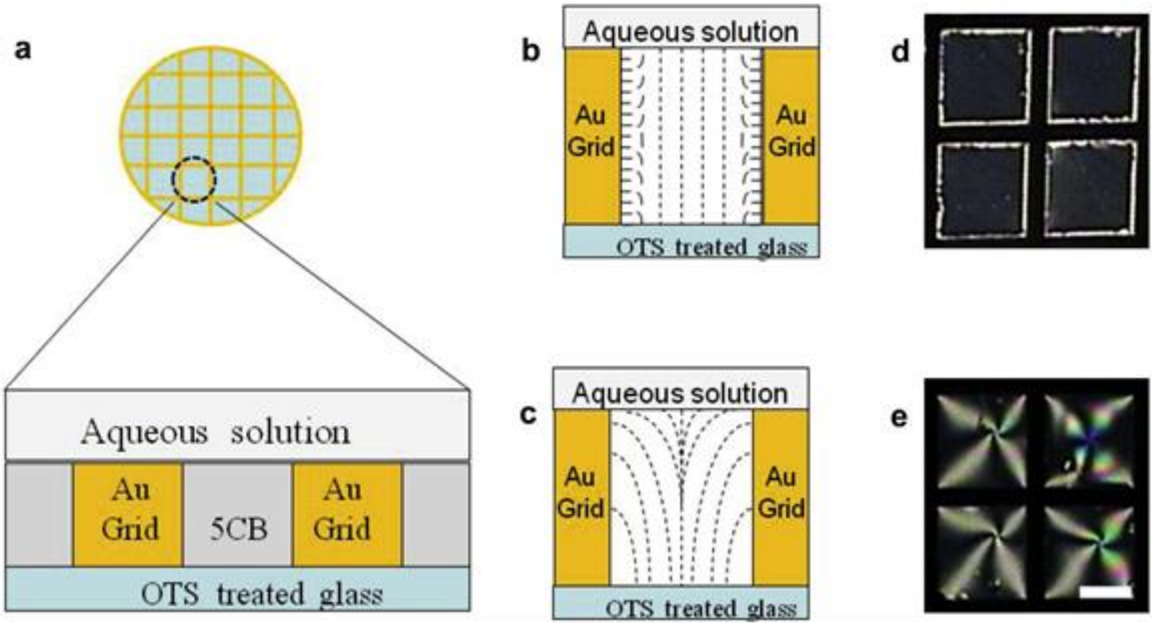

Figure 1.8 Schematic of the LC-based sensor (a) sensing mechanism of the LCs reorientation associated with the reaction of dodecyl -d-glucopyranoside by cellulase at the aqueous/LC interface: perpendicular (b) planar (c) states. The corresponding images combined to the orientation of LCs: black (d) bright (e) appearances [18].

Liquid crystal molecules are applied on DMOAP coated glass substrate which has TEM grids and that glass substrate is analyzed under polarized optical microscope. If the liquid crystal molecules are not aligned completely perpendicular then some leakage of light will happen [18].

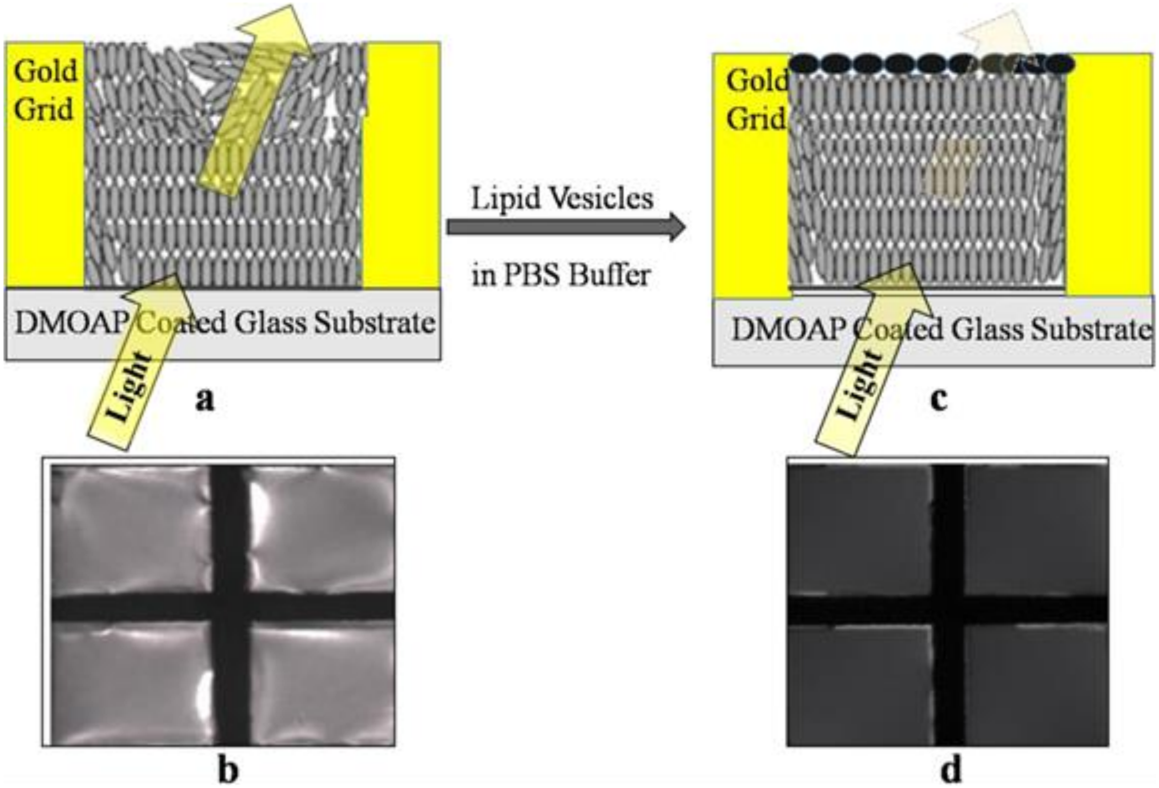

Figure 1.9 Principal of LC-based sensor (a) 5CB partially aligned in gold grids, also showing light transmission; (b) optical image of partially aligned 5CB observed under optical microscope; (c) 5CB fully aligned in gold grids, also showing light blocking; (d) Optical image of fully aligned 5CB observed under optical microscope [19].

1.6. Whatman® Anodisc Inorganic Membranes

These are commercially available membranes which have ordered AAO channels having pore size of 200nm. It is used in various types of filtration applications such as bacterial analysis using light microscope and high-performance liquid chromatography mobile phase filtration process.

1.7. Problem Statement

The use of TEM gold grid chambers for sensing applications using liquid molecules is very expensive and complex because it requires functionalization of DMOAP which is a very sophisticated process to handle. These TEM gold grid channels should be replaced by some other economical sensing chamber. One solution to this problem is that TEM gold grid chambers can be replaced by anodic aluminum oxide channels which are very economical as compared to TEM gold grids. Our project is to develop anodic aluminum oxide on aluminum substrate, optimize different parameters of anodization and finally to grow liquid crystals in AAO channels which can be used for sensing applications.

Chapter-2: Literature Review

Different scientists have done worked on the anodization of aluminum in different electrolytes to check the property of aluminum which could help in corrosion protection. This study is carried out mostly by the help of scanning electron microscopy and some other scanning machines which will be discussed later.

Jeiwu Cui. [4] Have studied this process of anodization by using phosphoric acid as an electrolyte at different temperatures for different time. He observed that small pore diameters were obtained in phosphoric acid. Top and bottom surface morphologies of the pores obtained by anodization in phosphoric acid is shown in Fig 2.1

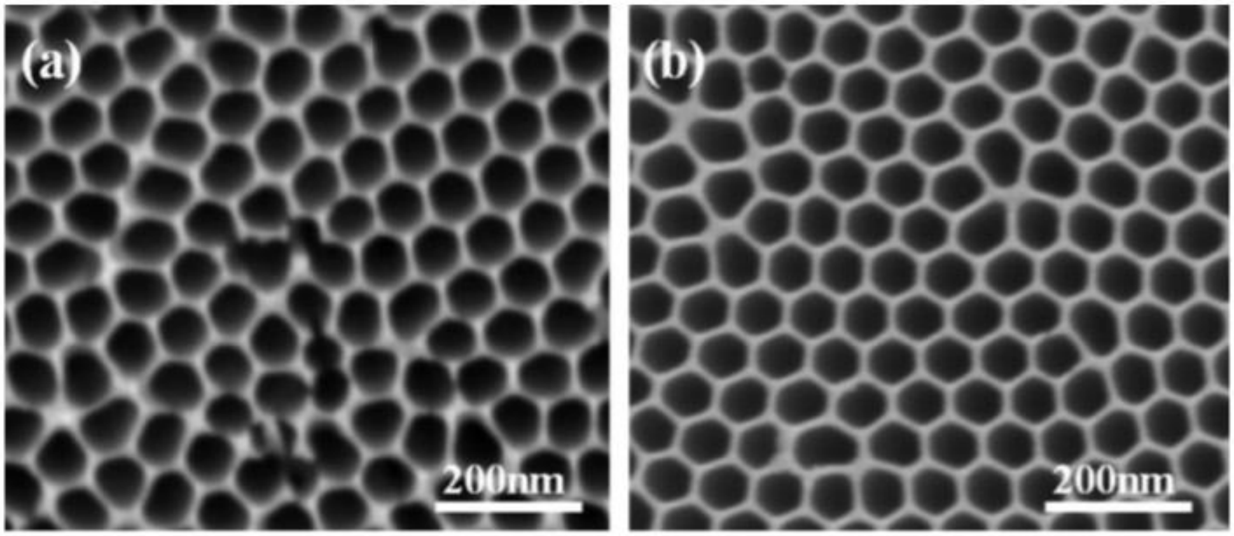

Figure2.1 SEM images of AAO immersed in 5 wt% $H3PO4$ for 35 min at 40^oC. (a) Top view. (b) Bottom view [4].

He prepared this porous alumina by using a pure aluminum foil and it is seen that results obtained by using pure aluminum foil are better as compared to the aluminum foil which is not pure.

2.1. Two step Anodization

J. H. Yuan. [9] Formed the perfect and regular pores in aluminum foil by using two step anodization process. In this process polishing and annealing of the foil is not important but simple oxide or grease removal, present on the surface of aluminum is necessary which can be done by dipping in 5wt% NaOH for 5 mins. This will removal any of the unnecessary particles present on the surface. The schematic representation showing the two step anodization is represented in figure 2.2.

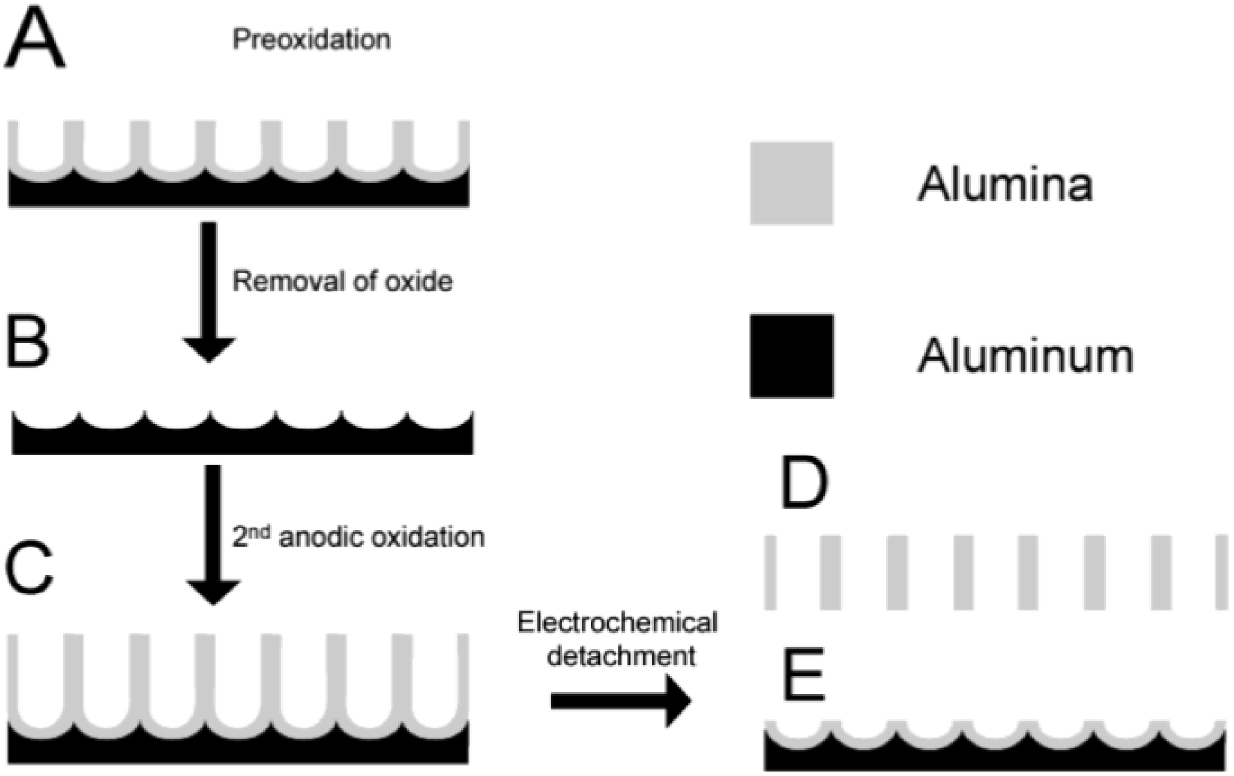

Figure2.2 Schematic representation showing the fabrication of porous alumina by two step anodization. (A) Formation of porous alumina after first anodization; (B) this part shows the removal of porous alumina formed in first anodization; (C) Formation of perfect and ordered pores by using second anodization process; (D) Free-standing porous anodic alumina; (E) Structure obtained after electrical detachment of porous anodic alumina [9].

But later he found that by annealing and electrical polishing further increase the perfection of pores because annealing causes the removal of stresses present in the foil, as these stresses are the possible burning points of the foil. So it is helpful if annealing of foil is performed before the anodization process.

2.2. Pore formation process

AAO process depends on current vs time profile which helps us to understand the process of anodization. The process of anodization is also depends upon the type, pH and concentration of electrolyte. Further factors on which this process depends involves temperature, time, voltage and surface conditions. Figure 2.3 shows the current vs time profile of anodization process.

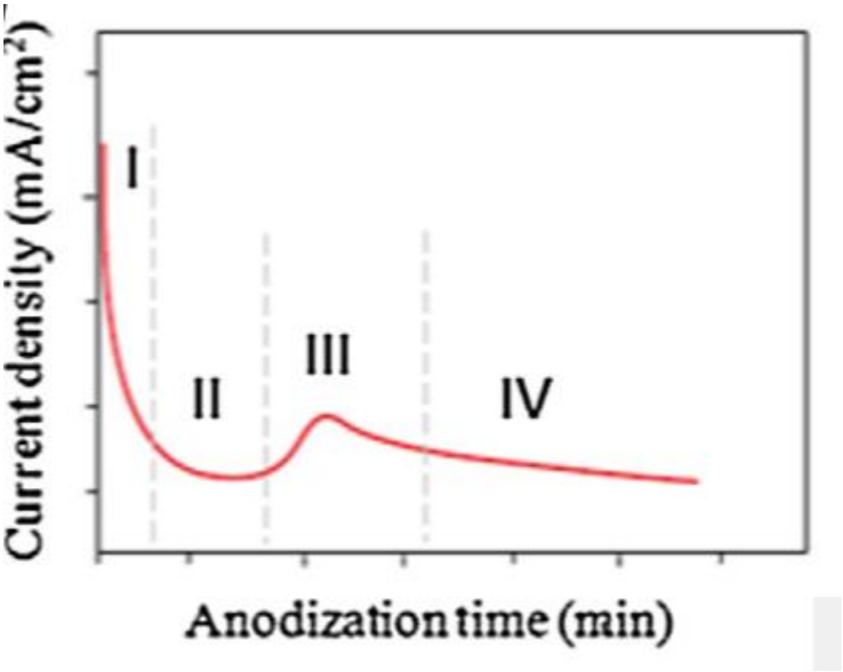

Figure2.3 Schematic representation showing the kinetics of anodization process [3].

Following are the stages shown in Fig 2.3.

I. Formation of oxide layer
II. Initiation of pore on oxide surface
   a. Formation of pore
   b. Growth of the pore

Now we discuss the formation of porous anodic alumina with the stages of pore formation. Figure 2.4 shows all the four stages.

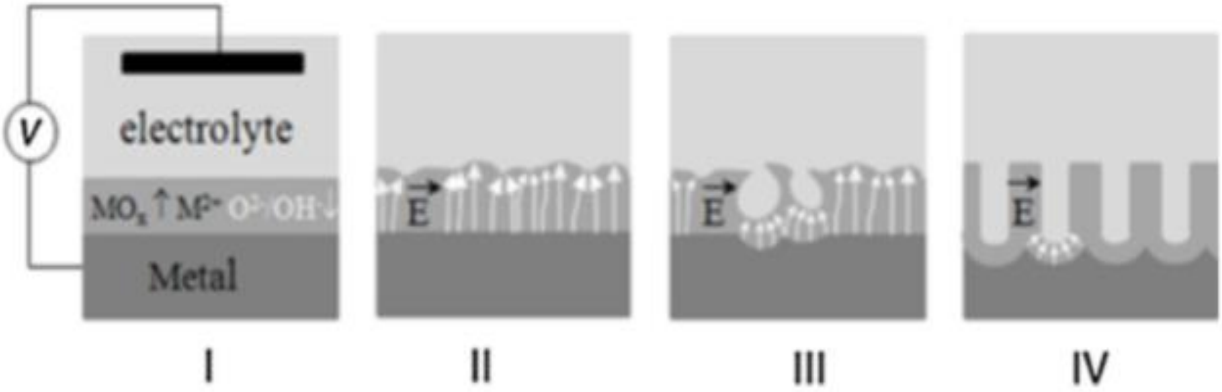

Figure2.4 Schematic showing the stages of pore formation [3].

We are going to discuss these stages one by one.

2.2.1. Oxide formation

When the anodization process starts the first step is the formation of compact and uniform oxide layer on the surface of aluminum. This layer forms under the constant voltage condition. Fig 2.3 and Fig 2.4 shows this stage. Once this layer forms the current density drops rapidly.

2.2.2. Initiation of pores

This stage involves the distribution of electric field on the oxide-electrolyte interface. As we know distribution of electric field depends on the inhomogeneities and surface roughness which leads to focusing of electric field in the interface which results in initiation of pores as shown in figure 2.3 and figure 2.4.

2.2.3. Formation of pore

As electric field focused on the interface this results in electric-field-dissolution of oxide layer takes place which helps in the formation of localized pores and this formation produces sites for further pore growth. This formation of pore in shown in figure 2.3 and figure 2.4. Initial pore formation is also shown in figure 2.5.

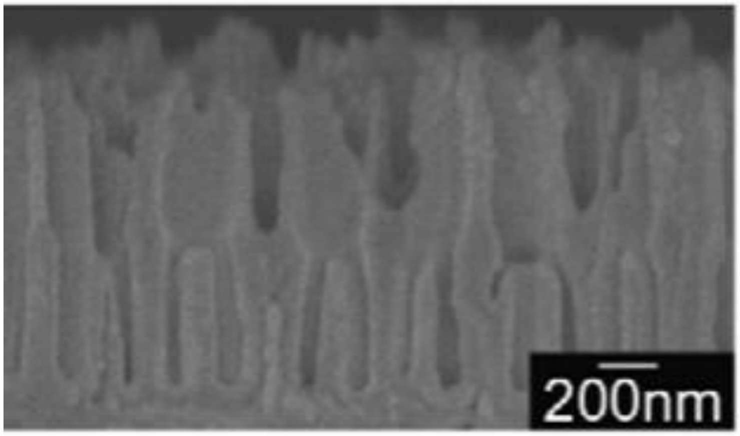

Figure2.5 Initial pore formation [3].

2.2.4. Growth of pores

Pores start to grow as the ionic migration increases which helps to increase in current density. And increase in current density occurs until pores cover the whole surface. At this stage of anodization pores are not uniform and if we more time to the process this will help them to achieve high regularity. This stage involves competition between oxide dissolution and oxide growth and finally growth of pores reaches some steady state and uniform pores formation occurs.

2.3. Processing parameters

These are the parameters on which the process of anodization actually depends. This involves electrolyte, voltage and pore size.

2.3.1. Pore size

A.Belwalker. [6] studied the pore size in 5 wt% sulfuric acid at 12.5 V and 2.7 wt% oxalic acid at 40 V. Table 2 and table 3 shows the pore size distribution with respect to voltage and concentration of electrolyte.

Table 2.1: Pore size of AAO membrane produced by 2.7 wt% oxalic acid at 30 and 40V at 0oC [6].

Concentration of oxalic acid (wt%)	Pore size (nm) DC voltage	
	30	40
2.7	18.6 ± 2.9	33.6 ± 7.6

Table 2.2: Pore size AAO tubular membranes produced by 3, 5, 7, 10 and 20 wt% sulfuric acid at different voltage and at 0oC [6]

Concentration of sulfuric acid	Pore size (nm), DC voltage(V)		
	12.5	15	20
3	19.9 ± 1.9	21.9 ± 1.8	24 ± 2.5
5	19.1 ± 1.9	21.4 ± 0.8	
7	19 ± 0.5		
10	18.4 ± 5.6		
20	13.7 ± 7.8		

As seen from the above table 2 increase in voltage results increase in pore size and similar behavior is observed in case of sulfuric acid.

2.3.2. Inter-pore distance

Interpore distance is another important factor in anodization process. Table 3 shows the Interpore distance when the wt% of sulfuric acid changes [6].

Table 2.3: Inter-pore distance of AAO produced at different concentration and variable voltage at 0oC [6].

Concentration of sulfuric acid (wt%)	Interpore distance (nm), DC Voltage (V)		
	12.5V	15V	20V
3	32.7 ± 2.8	36.4 ± 1.6	45.4 ± 8
5	31.9 ± 3.2	38.8 ± 0.4	
7	31.8 ± 2.9		
10	32.6 ± 4.7		
20	29.9 ± 2.4		

Table 2.4: Inter-pore distance of alumina foil anodized in 2.7wt% oxalic acid at different voltage.

Concentration of oxalic acid (wt%)	Interpore distance (nm), DC voltage (V)	
	30 V	40 V
2.7	65.1 ± 6.5	80.5 ± 3.2

2.3.3. Thickness

Here we are going to discuss the relationship between thickness of tubular membrane wall and second anodization time. Figure 2.6 shows the graph of such a relation.

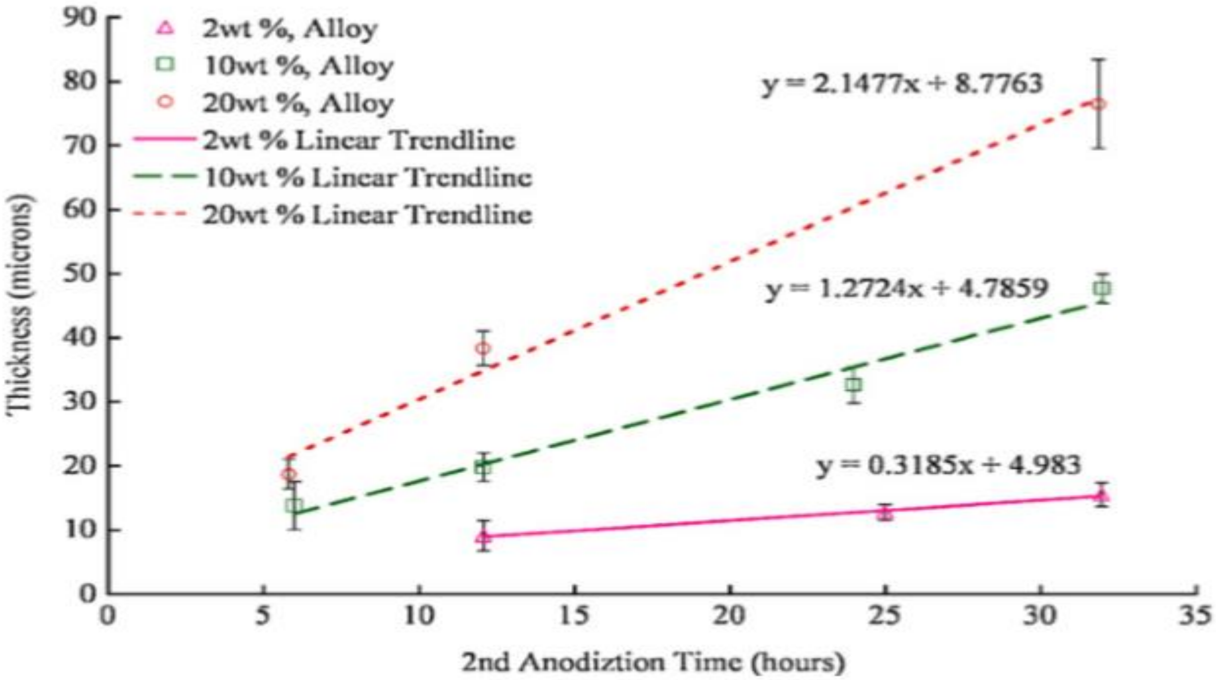

Figure 2.6 Variation of membrane thickness with respect to time [6].

As seen from figure 2.6 when anodized in 2, 10 and 20 wt% sulfuric acid and when anodization time increases from 2 to 32h, the thickness of the tubular membrane also increased.

2.4. Applications Overview

Ordered porous structure is widely used in nature because of its wide variety of applications in different fields of science.

Most significant features of these structures are the multifunctional properties in the charge transport, ion exchange, signaling, gas adsorption etc. This is basically because of large amount of surface area present just because of the porous structure. Due to its wide properties very limited work is done in the field of bio-sensing and chemical sensing. The applications of these structures in the field of sensing provide motivation which is helping us to explore this structure.

Chapter-3
Experimental Procedure

3.1. Electrochemical Anodization setup

Multi component electrochemical setup has been used for the formation of porous anodic aluminum oxide (AAO). The most vital part of this setup is the DC power supply that is used to get the constant voltage in the range of 0 to 190V. Digital multimeter, thermometer, recirculation chiller to attain low temperature, magnetic/mechanical stirrer to control heat produced for high voltage experiment, inert electrode and other essential components are also used additionally. In order to get the plots of output current against applied voltage with respect to time, computer interface can be used. These plots are very helpful and critical for the study of AAO. Components are discussed in detail in the following paragraphs.

3.1.1. Power Supply

To get the voltage supply in the range of 40-60V, QPX 1200S power supply was used as shown in the figure 1. High voltage above 60V was obtained by using locally manufactured power supply.

Figure 3.1 Power Supply

3.1.2. Digital Multi-meter

To study the current vs time behavior, DMM of Uni-Trend (model= T 60-A) group was used as shown in the figure 2. Computer generates the current vs. time plots on the basis of data saved from multi-meter automatically. The range of 400mA- 10A was used for anodization experiment.

Figure 3.2 Uni-Trend T-60 Ampere Digital Multi-meter

3.1.3. Computer Interface

Computer interface records the data of multi-meter and generates the current vs. time plots as shown in the figure 3. It allows us to monitor the change in current with respect to time during the course of experiment. This monitoring of current with respect to time is very important for the study of growth of pores.

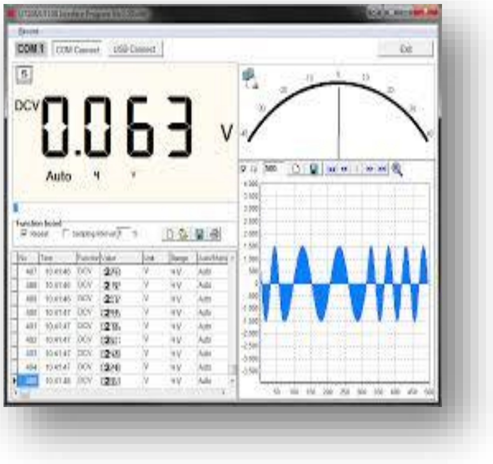

Figure 1.3 Computer Interface Screen

3.1.4. Magnetic Stirrer

Magnetic stirring is very crucial to avoid localized burning at the surface of sample during the anodization experiment. Both mechanical and magnetic means can be used for the purpose of stirring. For this purpose we used digital hotplate MSH20D wise stir as shown in the following figure 4.

Figure 3.4 Digital hotplate MSH20D wise magnetic stirrer.

3.1.5. Recirculating Chiller

To maintain low temperature in the anodization bath, pure anti freezing iso propanol was circulated using re-circulating chiller. For this purpose we used re circulating chiller of Haake F3 as shown in the figure 5. Small 1000ml glass beaker was used as an anodization bath which was placed in a relatively large 2000ml plastic jug, in which iso propanol was recalculated to maintain low temperature in the anodization bath. Inlet and outlet of the iso propanol in the jug were connected together to ensure recirculation. Thermometers were used to measure the temperature of electrolyte. The temperature of the electrolyte was always found less as compared to temperature that was set manually in control panel of the chiller.

Figure 3.5 Haake F3 Recirculating Chiller

3.1.6. Anode

Aluminum foil of size of 15 cm long and 4cm wide is used as anode for most of the experiments. We have also used 0.5mm thick sheet of aluminum for some experiments as an anode.

3.1.7. Cathode

We used lead as a cathode because of its inert properties for electrochemical processes.

3.1.8. Electrolyte

Electrolyte is a solution that is used in the electrochemical process. It provides charges to electrodes and acts as medium for the migration of charges as well. We have used two kinds of electrolytes:-

3.1.8.1 0.3 M oxalic acid:

It was prepared by adding 9.058g of sold COOH in 100ml of water.

3.1.8.2 5 vol. percent phosphoric acid:

It was prepared by adding 50 ml of phosphoric acid into 1 liter water. Phosphoric acid is used for the experiments done at high voltage as compared to experiments done at low voltage with oxalic acid.

3.2. Experiment Steps

3.2.1 Sample Preparation

3.2.1.1 Annealing

Aluminum sample was annealed in a muffle furnace at 400 degree centigrade and for 5 hours of soaking time. Annealing was done to remove internal stresses and to prevent burning and cracks.

3.2.1.2. Electro-polishing

After annealing, the sample was electro polished in “2 weight %” [8] NaOH and was rinsed afterwards with water.

3.2.1.3. First Anodization

First anodization is done for one hour while using different voltages in the range of 0-60 for both 0.3 M oxalic acid and 5volume% phosphoric acid.

3.2.1.4. Pore Widening

Pore widening is done after first anodization to increase the size of pores. It was done by dipping samples in 5volume % phosphoric acid for 30 minutes.

3.2.1.5. 2nd Anodization

2nd anodization is done for 2-3 hours after pore widening. It is done for the further growth of pores. It is done in the range of 0-60 V for both oxalic and phosphoric acid.

3.3. Experimental Scheme

Our Initial experiments were unsuccessful, due to the burning of our sample. This was probably due to the improper sample preparation. After doing proper sample preparation experiments we achieved better results from the experiments, details of which are shown in the following scheme.

Table 3.1

S.NO	Electrolyte	Time(h)		Temperature (^{o}C)	Voltage
		1st	2nd		
1.	0.3 M oxalic acid	1		10	33
2.		1		-7	20
3.		1		-5	25
4.	5 vol.%	1		-5	30

	phosphoric acid				
5.	0.3 M oxalic acid	1		-3	40
6.		1	2	0	40
7.		1		-2	40
8.		2		-2	60
9.	5 vol.% phosphoric acid	1		0	60
1o.		2.5		-5	60
11.		3		-2	50
12.		3		-2	70
13.		1		-3	60

3.4. Anodization Bath

A 1000 ml beaker was used as an anodization cell, which was placed in 2000 ml beaker (plastic jug) that is used for the recirculation of anti-freezing iso-propanol solution and holding of anodization. Anodization cell consisted of a thermometer, magnetic stirrer bar, an anode, a cathode as shown in the following figure. Thermometer was installed in the anodization cell to monitor temperature changes during the course of experimentation. Magnetic stirrer was used to minimize heat generation at the surface of aluminum. Digital ammeter was connected to the computer interface to record the current vs. time plots. Voltmeter was connected to the cell to observe voltage changes.

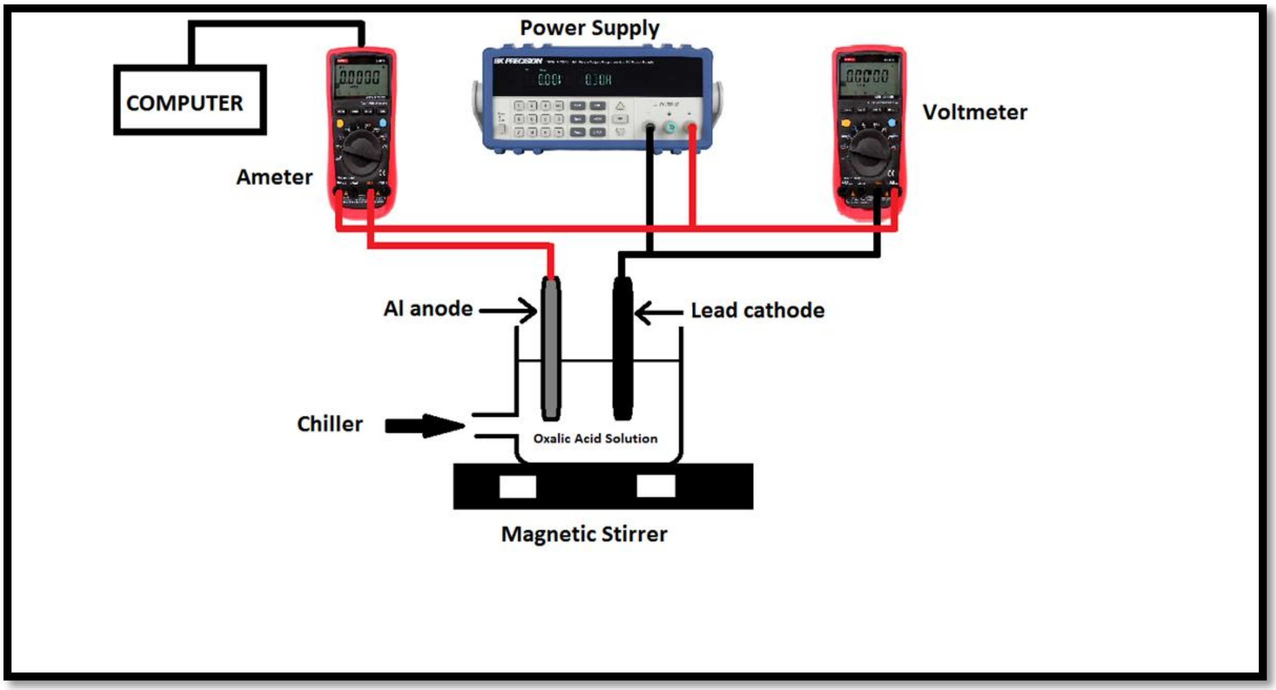

Figure 3.6 Experimental Setup

Chapter-4
Results and Discussions

4.1. SEM images and current profiles

To check all the results our whole experimentation is divided into different steps. We are going to discuss SEM images and current profiles of our experiments.

4.1.1. Surface analysis of AAO obtained at 60V

When we perform our experiment in 5 vol% phosphoric acid at a voltage of 60V and temperature given was -5^{o}C so that the produced heat can be dissipated easily. Experiment conditions are also given in table below.

Table 4.1 shows the parameters of AP

Sample	Electrolyte	Time (hrs)	Temperature (^{o}C)	DC voltage	Pore size in nm
AO2	5 vol% phosphoric acid	2.5	-5^{o}C	60	20-40nm

Below figures shows the sample obtained, after performing anodization process.

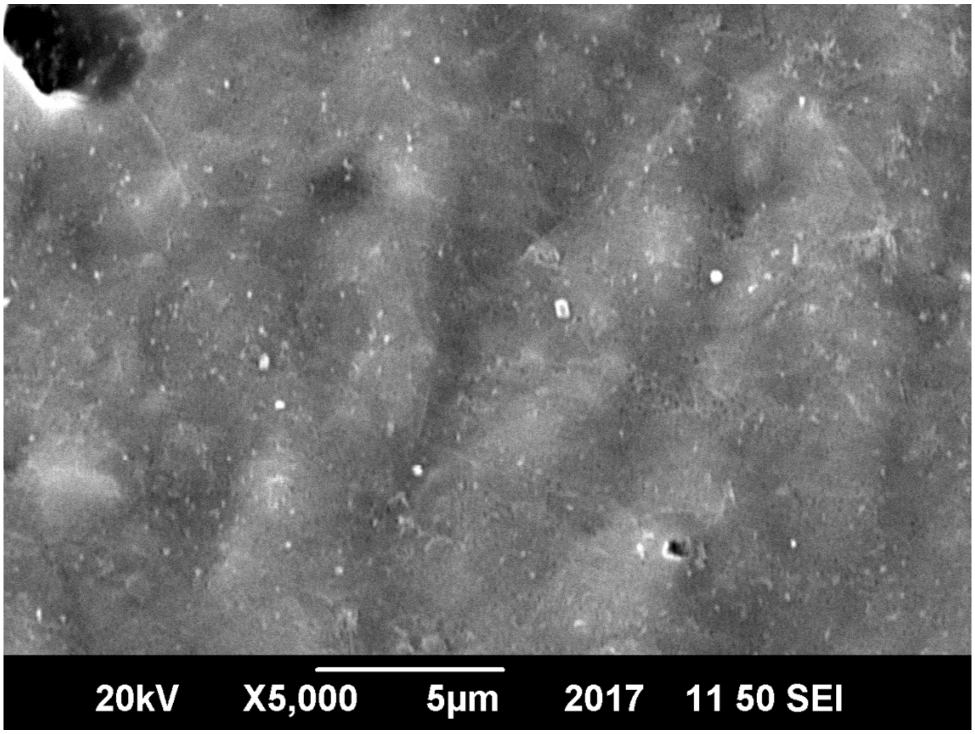

Figure 4.1 SEM image of anodized aluminum foil, anodized at 60V and in 5 Vol% phosphoric acid and image is taken at a magnification of 5000X

Figure 4.1 shows the SEM image at a magnification of 5000x. As a magnification is low so we cannot see any pore present. As seen the surface of the alumina contain some cavities, these are some intermetallic compound which form during the process. These can be eliminated by using a foil of high purity and by performing pre-treatments.

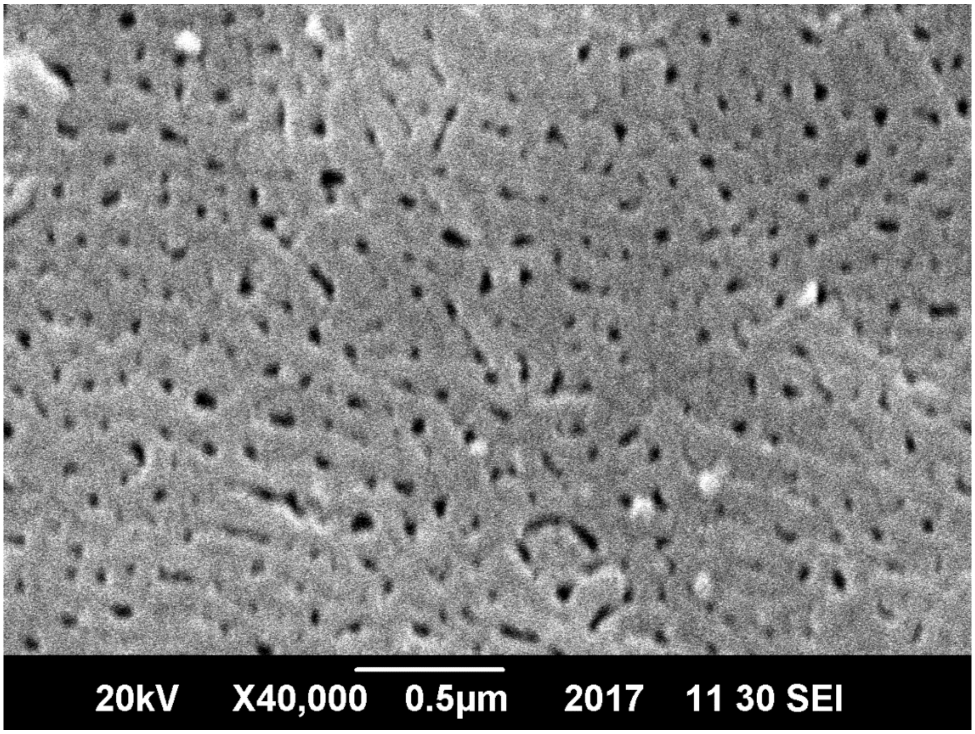

Figure 4.2 SEM image at magnification of 40000X

Figure 4.2 shows the SEM image of same sample anodized at 60V in phosphoric acid but image was taken at higher magnification of 40000x. This shows the porous structure on the surface. As it can be seen pores are continuous and regular.

4.1.2. Surface analysis of AAO anodized at 50V

We performed the anodization process in 5 vol% phosphoric acid at a temperature of -2^{o}C when the given voltage is 50V. Table 4.2 shows the experimental conditions.

Table 4.2 shows the AP parameters

Sample	Electrolyte	Time (hrs)	Temperature (°C)	DC voltage	Pore size in nm
AO2	5 vol% phosphoric acid	3	-2°C	50	20-40nm

Below are the two figures of the sample anodized at 50V and at a temperature of -2°C

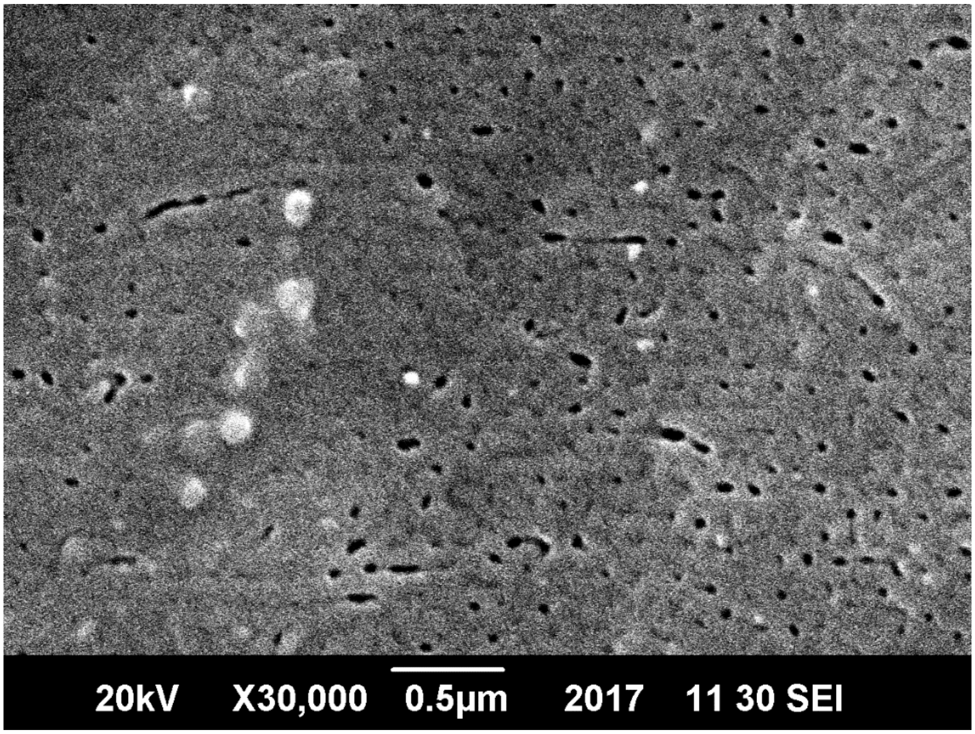

Figure 4. 3 SEM micrograph of AAO at a magnification of 30000X

As shown in figure 4.3 some porous structure is obtained when anodization is performed at a voltage of 50V. Figure also shows cavities which is intermetallic compound.

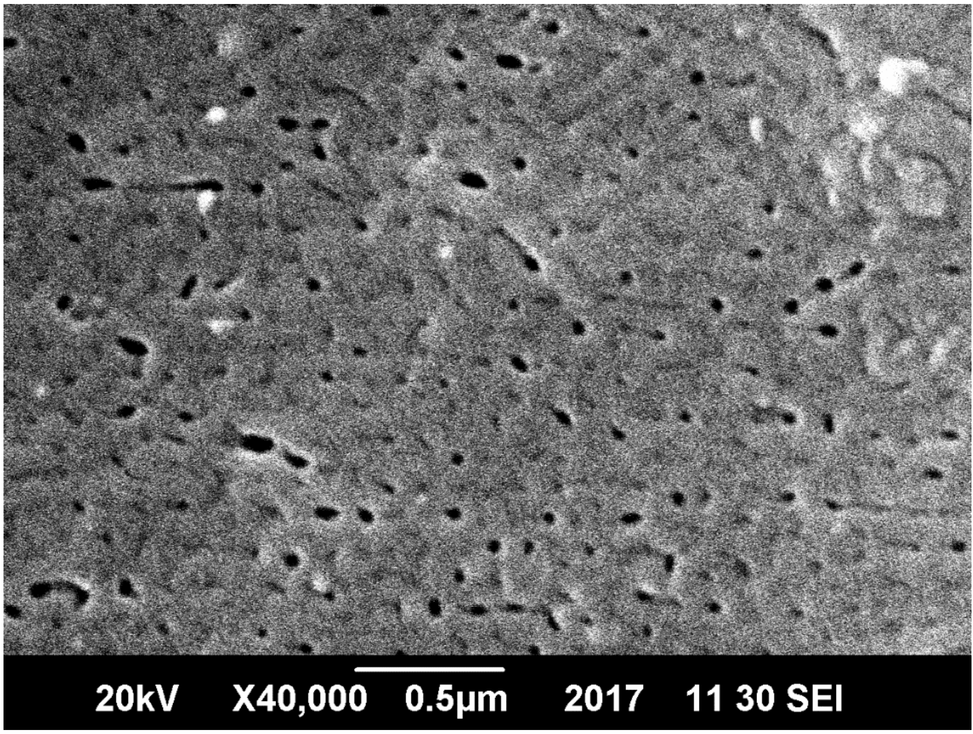

3.

Figure 4.4 SEM micrograph at a magnification of 40000X

Figure 4.4 shows the porous alumina and when we measured the diameter of these pores it comes out to be 20-40 nm. As seen that diameter of the pores varies which is due to variation in the temperature.

4.1.3. Sample analysis of AAO at 70V

This sample is anodized in 5 vol% phosphoric acid at a temperature of -2^{o}C when the voltage applied was 70V. Table 4.3 also shows the experimental conditions.

Table 4.3 shows the experimental parameters

Sample	Electrolyte	Time (hrs)	Temperature (^{o}C)	DC voltage	Pore size in nm
AO2	5 vol% phosphoric acid	3	-2^{o}C	70	25-55nm

As the voltage is high so some points of the sample were burnt due to production of large amount of heat. Figure 4.5 shows the burnt samples

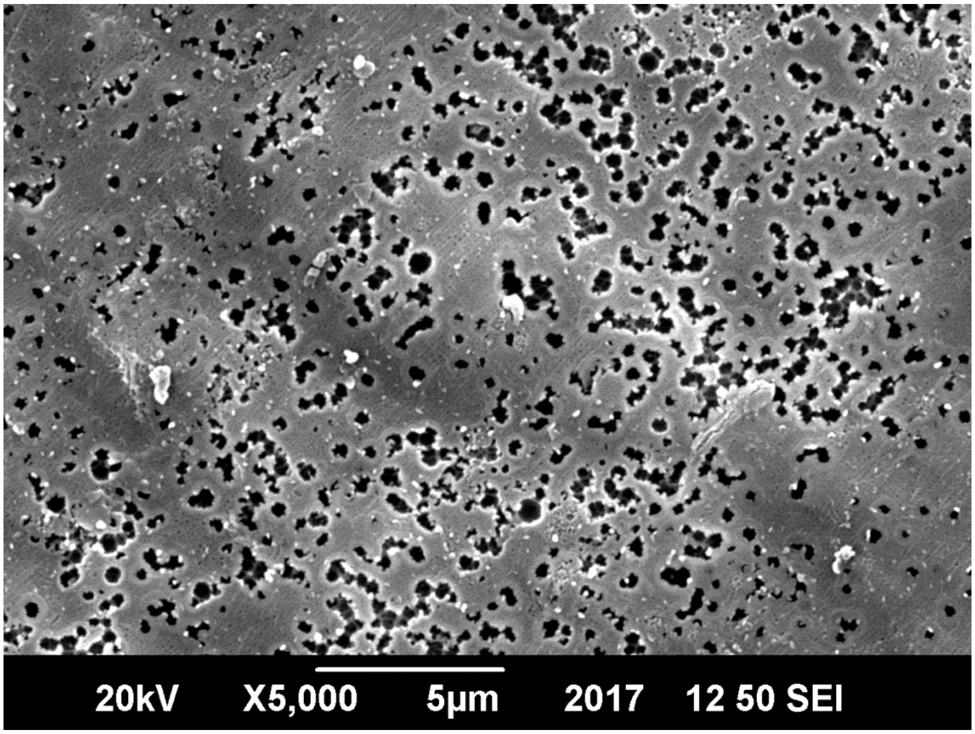

Figure 4.5 SEM image of burnt sample at a magnification of 5000X

Figure 4.5 shows the sample which is burnt. This burning of sample is due to overheating of sample because temperature provided is not enough to dissipate properly the produced heat.

When we further magnify our sample we can see some pores present at a point which is not burnt as shown in figure 4.6.

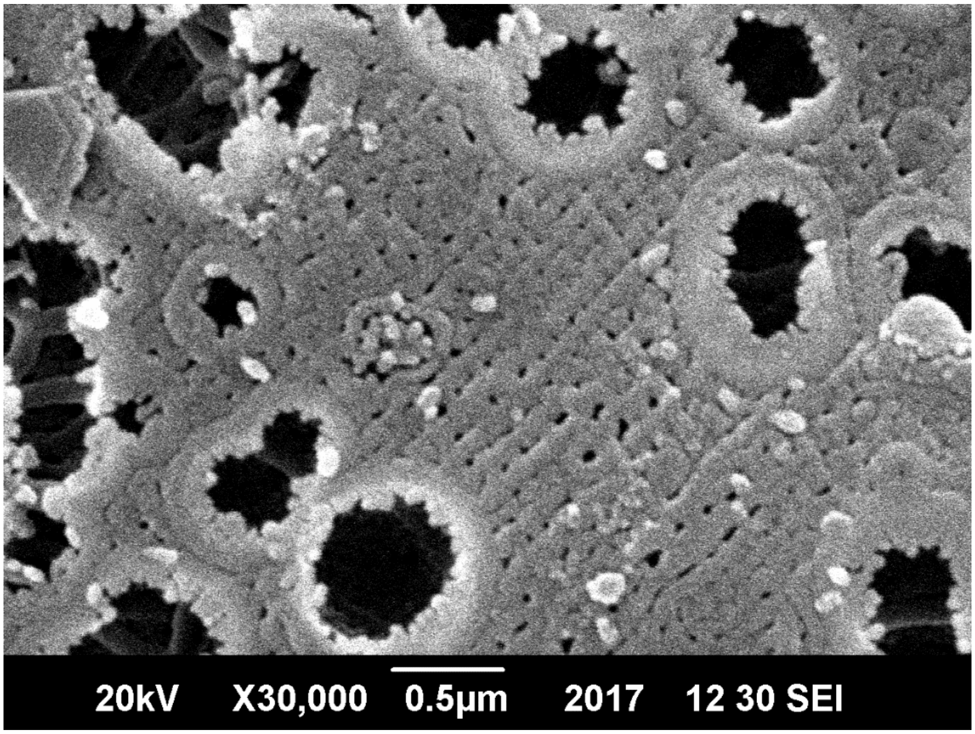

Figure 4.6 SEM image of sample at magnification of 30,000X

Above figure shows the porous structure at some points whereas when these burnt points were further magnified we see some porous and irregular structure inside these burning points.

4.1.4. Surface analysis of AAO obtained at 25V

Randomly organized and relatively small pores are obtained at 25V in 0.3M oxalic acid as shown in figure 4.4. The parameters for the anodization done at these conditions are given in the following table.

Table 4.4 Parameters for AO performed at 25V

Sample	Electrolyte	Time(hour) 1st	Temperature	DC Voltage
1.	0.3 M oxalic acid	1	-5	25

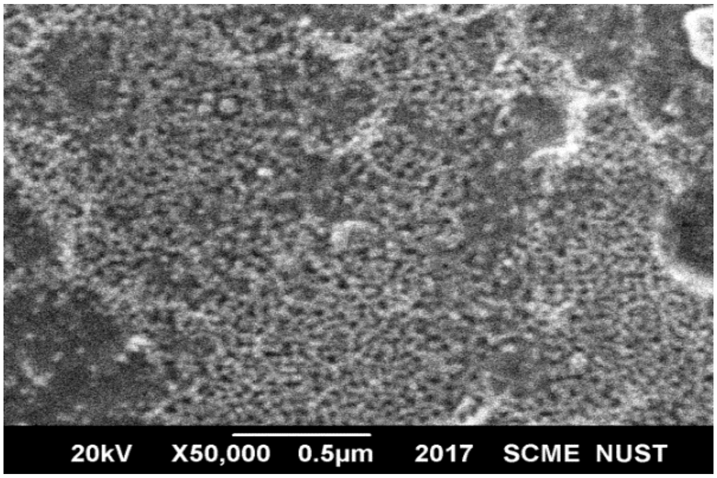

Figure 4.7 SEM micrographs for anodization of aluminum foil performed at 25V in 0.3M oxalic acid at magnification of 50000X.

Figure 4.7 shows randomly organized and small size porous network of anodic aluminum oxide. Regularity, continuity and homogeneity is lacking this porous network of anodic aluminum oxide. Also the whitish areas in the figure are due to the formation inter-metallic compound. Formation of the inter-metallic compounds can be minimized by pretreatments and using high purity aluminum foil.

The current vs. time profile for this experiment is shown in the following figure 4.8.

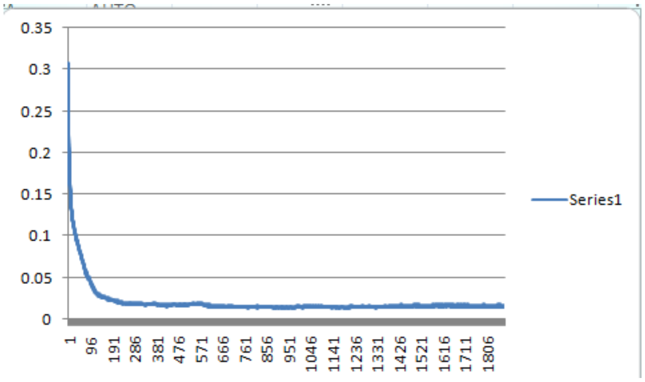

Figure 4.8 Current profile

Above figure depicts the formation of porous network of anodic aluminum oxide. Initially current density decreases due to the formation of insulating aluminum oxide layer but becomes constant after certain time, which shows the formation and growth of pores.

4.1.5. Surface Analysis of AAO obtained at 40V

This experiment was done at relatively high voltage i.e 40V. The voltage was increased to increase the pore size. High voltage produces heat at the surface of aluminum. To minimize the heat effect temperature was kept to 0°C using the recalculating chiller. Parameters used for this experiment are shown in the following figure.

Table 4.5 Parameters for AO performed at 40V

Sample	Electrolyte	Time(hour) 1st	Temperature	DC Voltage	Result
1.	0.3 M oxalic acid	1	0	40	Burnt

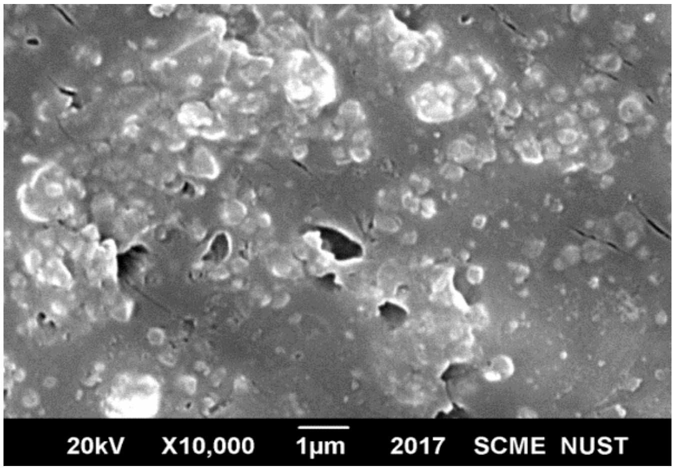

Figure 4.9 SEM micrograph of anodization of Aluminum foil at 40V, in 0.3 M oxalic acid

As it can be seen from the above figure that sample got burnt for the experiment done at 40V and 0°C. Aluminum was not anodized under these conditions due to the overheating. Overheating was probably the result of high voltage, improper pretreatments and to high temperature. Overheating also occurred due to the automatic shutdown of the recalculating chiller after having achieved certain specific temperature after certain time which led to the lowering of temperature of the electrolyte. Resultantly temperature was not enough to reduce the cracks developed at the surface of aluminum. We could also see the presence of inter-metallic compounds in the figure. These inter metallic compounds can be reduced by doing proper pretreatments and by using high purity aluminum foil.

The current vs. time profile for this experiment is shown in the following figure 4.10.

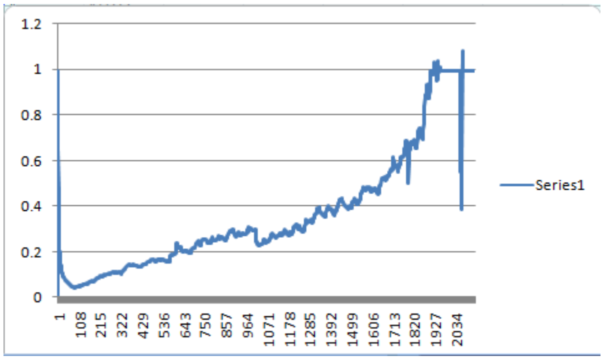

Figure 4.10 Burnt sample profile after first anodization.

Figure shows the current vs. time profile for this experiment. After decreasing, the rise in the current shows the start of the burning which continues as the current continues to increase.

4.1.6. Surface Analysis of AAO obtained at 40V

This experiment is also done at 40V. The high voltage produces large amount of heat at the surface of the sample. To minimize the heat effect, temperature is kept to 0^0 C. The parameters for this experiment are shown in the following figure.

Table 4.6 Parameters for anodization performed at 40V in 0.3M oxalic acid.

Sample	Electrolyte	Time(hour)		Temperature	DC Voltage	Result
		First	Second			
1.	0.3 M oxalic acid	1	1	0	40	Burnt

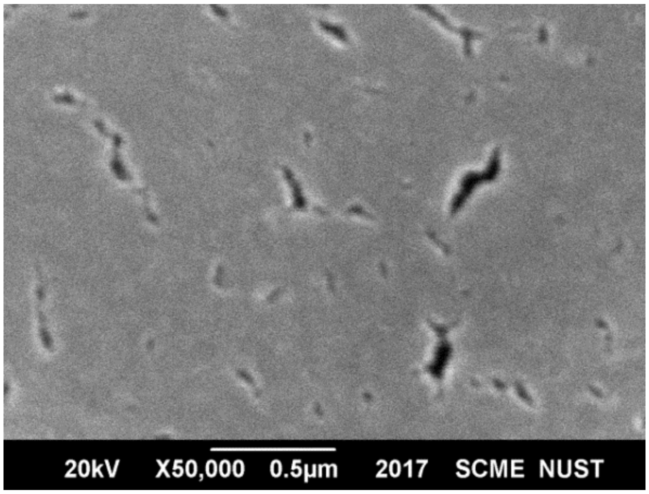

Figure 4.11 SEM micrograph for anodization of Aluminum foil at 40V, in 0.3 M oxalic acid and at the magnification of 50000X

It can be seen from the above figure that during the second anodiation, sample got burnt for the experiment done at 40V and 0^{o}C. Aluminum was not anodized under these conditions due to the overheating. Overheating was probably the result of high voltage, improper pretreatments and to high temperature. Overheating also occurred due to the automatic shut down of the recalculating chiller after having achieved certain specific temperature after certain time which led to the lowering of temperature of the electrolyte. Resultantly temperature was not enough to reduce the cracks developed at the surface of aluminum.

The current vs. time profile for this experiment is shown following in figure 4.12

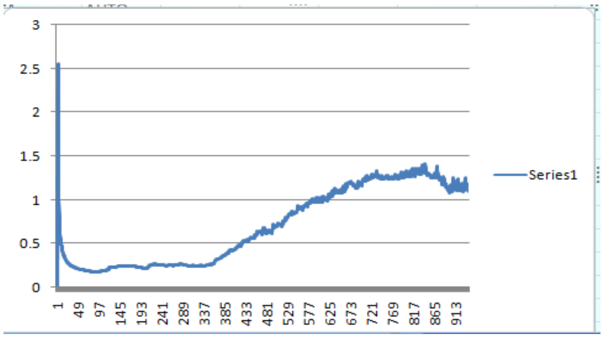

Figure 4.12 Burnt sample profile after 2nd anodization.

The current vs. time profile for this experiment is shown in above figure. After decreasing initially, current becomes constant which shows the growth of pores of AAO and finally the rise in the current shows the start of the burning which continues as the current continues to increase. The current increases at fewer rates as compared to the current increase for the first anodization.

4.2. Future perspective

After performing series of experiments and by working on results obtained from these experiments we see various parameters come into play with the help of which we can change our pore length and diameter depending upon the application. To move forward in the utilization of AAO we recommend the new researchers to work in the following directions:

1. Formation of porous membrane of certain pore size on thin film will help in filtration at nanoscale.

2. Liquid crystal based sensing applications.

5. Conclusions

- Use of low voltage will help to achieve pores of less diameter whereas to get pores of large diameter we need to increase our voltage. This applied voltage varies according to type of electrolyte.
- Magnetic stirrer will help to maintain a constant temperature in the cell and it also helps to obtain highly ordered pores.
- To compensate the local heat generated during the process we need to maintain our cell temperature between -2oC to -7oC.
- Annealing and pre-treatment is necessary to remove any of the internal stresses present in the sample because these stresses increase the probability of burning of the foil.
- As the purity level of the sample increase more ordered pores obtained because impurity forms intermetallic compounds on the sample

References

[1] Huiling Lv, Y.S., Liu Cao, Chunyan Yang, Huapeng Xiao, Shaoyu Zhang, Anodization of dual-layer laminated aluminum foils: A facile route to through-hole porous anodic alumina templates. 2014.

[2] Junping Zhang, J.E.K., David L. Carroll, Controllable fabrication of porous alumina templates for nanostructures synthesis Materials Chemistry and Physics, 2010.

[3] Abdul Mutalib Md Jani, D.L., Nicholas H. Voelcker, Nanoporous anodic aluminum oxide: Advances in surface engineering and emerging applications. Progress in Materials Science, 2013.

[4] Jiewu Cui, Y.W., Yan Wang, Hongmei Zheng, Guangqing Xu, Xinyi Zhang, A facile and efficient approach for pore-opening detection of anodic aluminum oxide membranes. applied surface science, 2012.

[5] P. Chowdury, M.K., Harish Barshilia Effect of process parameters on growth rate and diameter of nano-porous alumina templates. Bulletin of materials science, 2011.

[6] Belwalkar, A., Effect of processing parameters on pore structure and thickness of anodic aluminum oxide (AAO) tubular membranes. 2008.

[7] Abel Santos , T.K., Dusan Losic Nanoporous Anodic Alumina: A Versatile Platform for Optical Biosensors. 2014.

[8] Yuanjing Lin, Q.L., Xue Liu, Yuan Gao, Jin He, Wenli Wang, Zhiyong Fan, A Highly Controllable Electrochemical Anodization Process to Fabricate Porous Anodic Aluminum Oxide Membrane. Nanoscale Research Letters, 2015.

[9] J. H. Yuan, F.Y.H., D. C. Sun, X. H. Xia A Simple Method for Preparation of Through-Hole Porous Anodic Alumina Membran. 2004.

[10] Krissada Surawathanawises, X.C., Nanoporous anodic aluminum oxide with a long-range order and tunable cell sizes by phosphoric acid anodization on prepatterned substrates. National Institutes of Health, 2014.

[11] Chi Lu, Z.C., Anodic Aluminum Oxide-Based Nanostructures and Devices. 2011.

[12] Jin Shyong Lin, S.H.C., Ker Jer Huang, Chien Wan Hun, Chien Chon Chen, Challenges to Fabricate Large Size-Controllable Submicron-Structured Anodic-Aluminum-Oxide Film. Atlas Journal of Materials Science 2015.

[13] McCamley, M.K., Development of a Liquid Crystal Biosensor for the Detection of Endotoxin, in Division of Engineering. 2009, Brown University.

[14] Tsuyoshi MAEDA, K.H., Vertically Aligned Nematic Liquid Crystal on Anodic Porous Alumina. IOP Science, 2004.

[15] Tang, T.-T., Strong Vertical Alignment of Liquid Crystal on Porous Anodic Aluminum Oxide Film. JOURNAL OF DISPLAY TECHNOLOGY, 2009.

[16] Carlton, R.J., Chemical and biological sensing using liquid crystals. NIH, 2014

[17] Hong, C., NANOPOROUS ANODIC ALUMINUM OXIDE (NP-AAO) ALIGNMENT LAYER ON PET/ITO SUBSTRATE FOR FLEXIBLE LIQUID CRYSTAL DISPLAY APPLICATION 2011.

[18] Yi Wang, Q.H., Tongton Tian, Yan'an Gao, Li Yu, A liquid crystal-based sensor for the simple and sensitive detection of cellulase and cysteine. 2016.

[19] Zakir Hussain, F.Q., Muhammad Imran Ahmed, Adil Usman, Asim Riaz, Amna Didar Abbasi, Liquid Crystals Based Sensing Platform-Technological Aspects. Biosensors and Bioelectronics, 2016.